Available online at BCREC website: https://bcrec.id

Bulletin of Chemical Reaction Engineering & Catalysis, 16 (4) 2021, 804-815

Research Article

Photocatalytic Degradation of *Remazol Brilliant Blue R* and *Remazol Yellow FG* using TiO_2 doped Cd, Co, Mn

Candra Purnawan[1,*], Sayekti Wahyuningsih[2], Oktaviani Nur Aniza[1], Octaria Priwidya Sari[1]

[1]*Analytical Chemistry, Chemistry Department, FMIPA, Sebelas Maret University, Jl. Ir. Sutami 36A, Kentingan Surakarta 57126, Indonesia.*
[2]*Inorganic Chemistry, Chemistry Department, FMIPA, Sebelas Maret University, Jl. Ir. Sutami 36A, Kentingan Surakarta 57126, Indonesia.*

Received: 11th June 2021; Revised: 25th August 2021; Accepted: 26th August 2021
Available online: 31st August 2021; Published regularly: December 2021

Abstract

TiO_2 and TiO_2 doped Cd, Co, Mn (TiO_2-M) were synthesized with a sol-gel method, and the photocatalytic activity of *Remazol Brilliant Blue R* and *Remazol Yellow FG* has been conducted. TiO_2-M (Cd, Co, Mn) was synthesized with the mol Ti:M ratio of 3:1, and the materials were calcined at 300, 400, and 500 °C. The materials were characterized by X-ray Diffraction (XRD), Scanning Electron Microscopy-Energy Dispersive X-ray (SEM-EDX), and UV-Vis Reflectance. The XRD result shows that at the temperature of 300 °C TiO_2 and TiO_2-M formed tend to be amorphous. At 400 °C the anatase phase is formed, while at 500 °C the rutile phase begins to form. And overall, the crystallinity of TiO_2 is higher than metal-doped TiO_2. The UV-Vis Reflectance result showed that the bandgap energy of all doping materials (TiO_2-M) decreased. The larger the metal ion radius of dopant, the larger the crystal size obtained and then the higher the bandgap obtained. The results of SEM-EDX showed that the morphology of TiO_2 was spherical and regular, whereas the morphology of TiO_2-M had a smoother surface due to the influence of metal doping. Photocatalytic activity of TiO_2-M on *Remazol Brilliant Blue R* and Remazol Yellow FG was greater than TiO_2. The optimum pH of the solution was obtained at pH 5 and the optimum catalyst phase was obtained at the anatase phase. The percentages degradation for 30 min of *Remazol Brilliant Blue R* were 67.34% (TiO_2), 92.12% (TiO_2-Co), 85.47% (TiO_2-Mn), and 83.91% (TiO_2-Cd), while for *Remazol Yellow FG* they were 58.84% (TiO_2), 74.61% (TiO_2-Co), 67.93% (TiO_2-Mn) and 64.19% (TiO_2-Cd), respectively.

Keywords: Degradation; Remazol Brilliant Blue R; Remazol Yellow FG; TiO_2; TiO_2-M (Cd, Co, Mn)

How to Cite: C. Purnawan, S. Wahyuningsih, O.N. Aniza, O.P. Sari (2021). Photocatalytic Degradation of *Remazol Brilliant Blue R* and *Remazol Yellow FG* using TiO_2 doped Cd, Co, Mn. *Bulletin of Chemical Reaction Engineering & Catalysis*, 16(4), 804-815 (doi:10.9767/bcrec.16.4.11423.804-815)

Permalink/DOI: https://doi.org/10.9767/bcrec.16.4.11423.804-815

1. Introduction

The textile industry is one of the biggest sources of water pollution, with a large amount of dye waste [1]. The negative impacts of textile production are primarily derived from the dyeing process resulting in dye wastewater, which has a chromophore groups [2]. Dye waste disposed by the textile industry is a pollutant that may contaminate the environment. The waste is extremely harmful to the environment, especially the river ecosystem in Indonesia. They are stable, difficult to degrade, toxic, mutagenic, and carcinogenic [3,4]. Some of the dyes frequently applied in the textile industry are anionic dyes of *Remazol Brilliant Blue R* and *Remazol Yellow FG*. The two dyes provide bright colors on textile but due to the complex structure, reactive, and difficult to be biologically degraded. Dye

* Corresponding Author.
Email: candra_pr@staff.uns.ac.id (C. Purnawan);
Telp: +62-81227142177

waste has to be managed to prevent environmental pollution. To date, such a method of dye waste management as photodegradation has been developed. Photodegradation utilizes photocatalyst and ultraviolet rays whose energy is equivalent to or higher than the energy of the photocatalyst bandgap [5]. Some of the textile industry wastewater treatment that continuously developed to minimize waste pollution is photocatalyst and photoelectrocatalyst [6,7]. Several photocatalysts have been used to degrade *Remazol Brilliant Blue R* and *Remazol Yellow FG*. However, the degradation process often takes much time and a large amount of light energy, such as UV lamps, making it less effective and efficient. Photocatalytic degradation of *Remazol Brilliant Blue R* under ultraviolet irradiation (UV light) was examined and ~80% degradation was achieved but in 120 min (2 h) by using Nanostructured bio-photocatalyst hydroxyapatite (HAp) [8]. C-doped TiO_2 photocatalyst did not only achieve discoloration of *Remazol Brilliant Blue R* but also removed 70% of organic carbon but in 6.5 hour [9]. The nickel-based catalyst ($EGNiO_{1000}$) shows excellent photoactivity which degraded around 90.0% of *Remazol Brilliant Blue R* but in 1.5 hour using florescent lamp [10]. Catalyst of Fe_2O_3 intercalated bentonite has degraded remazol brilliant blue 98.02% but in 2 hours using UV light [11]. The iron oxide nanoparticle that was synthesized from leaf extract of Carica papaya plant showed efficient degradation ability against remazol yellow RR dye in the presence of sunlight about 77% but in 6 hours [12]. Removal of Remazol Yellow using Sn/SBA-15 catalyst was 58.2% [13]. The degradation of Remazol Yellow was reached 96% within 1 h using catalyst Polyaniline (PANI)-doped tin oxide-diatomite and UV lamp [14].

And today, TiO_2 is one of the most prospective catalyst with such advantages as long-term stability, easy to modify, cost-effectiveness, and non-toxicity [15]. However, the success of TiO_2 is still traded off by the large energy of the band gap (3.2 eV) and rapid recombination valence of electron-hole that decreases the photocatalytic activity [16]. Therefore, modification is needed to improve the photocatalytic activity of TiO_2. The limitation of TiO_2 can be improved by developing a TiO_2 composite with other semiconductor materials so it can absorb the visible light and avoid recombination [17,18]. Modification with transitional metal doping can decrease the energy of the band gap and reduce the process of electron-hole recombination so that the process of catalytic reaction at the TiO_2 surface can last longer [19]. Some applicable transitional metals include Cd, Co, and Mn.

The addition of metal ions to the TiO_2 crystal lattice results in changes in the crystal structure, crystal size and electronic properties of TiO_2. The addition of metal ions can reduce the crystallinity of TiO_2 because of the difference in radii and charge between metal ions and Ti^{4+} ions. Metal ions can inhibit crystal growth, causing the crystal size to become smaller. The addition of metal ions is also possible to reduce the band gap energy of TiO_2 which has an impact on increasing light absorption into the visible region [19]. It is possible for metal ions to enter the crystal lattice and substitute for Ti^{4+} ions which causes the formation of new energy levels so that it has an impact on decreasing the width of the band gap. The decrease in the band gap width will cause the photon energy used for electron excitation to be lower so that the band gap energy decreases. In addition, the addition of metal ions to TiO_2 acts as an electron trapper that can prevent electron-hole recombination so that it can increase its photocatalytic activity [20]. The addition of Co into TiO_2 causes a decrease in crystal size and a decrease in band gap energy thereby increasing its photocatalytic activity [21]. Changes in the crystal structure and electronic properties of TiO_2-M (M= Cd, Co, Mn) can be identified through characterization using XRD, SEM-EDX, and UV-Vis Reflectance spectrophotometer. And then, it's photocatalytic activity can be studied further.

To date, there has been no application of TiO_2-M (Cd, Co, Mn) catalyst for the degradation of anionic dyestuffs such as Remazol Brilliant Blue R and Remazol Yellow FG. Therefore, there needs to be a study to see the ability of the catalytic activity of TiO_2-M (Cd, Co, and Mn) in degrading the anionic dyes Remazol Brilliant Blue R and Remazol Yellow FG.

2. Materials and Methods

2.1 Equipment and Materials

The equipment had been used in the research were glassware (Pyrex), X-Ray Diffraction Spectrophotometer (Bruker D8 Advance), Spectrophotometer UV-Vis (Perkin Elmer Lambda 25), Scanning Electron Microscopy-Energy Dispersive X-Ray (JOEL JED-2300). While the materials used were Titanium (IV) Isopropoksida (TTIP) (Merck), glacial acetate acid (Merck), $CdSO_4.8H_2O$ (Merck), $CoSO_4.7H_2O$ (Merck), $MnSO_4.1H_2O$ (Merck), aquades, *Remazol Brilliant Blue R* and *Remazol Yellow FG*.

2.2 Synthesis of TiO_2

TTIP was hydrolyzed with glacial acetate acid solution (at 14 °C) with a ratio of 1:10 (v/v). The solution was stirred and heated at 90 °C. The formed gel was then heated in the oven at 150 °C for ±24 hours and calcined at different temperatures of 300, 400, and 500 °C for 2 hours.

2.3 Synthesis of TiO_2-M (Cd, Co, Mn)

TTIP was hydrolyzed with glacial acetate acid solution (14 °C) with a ratio of 1:10 (v/v). The solution was stirred and heated at 90 °C. The formed gel was then added to $CdSO_4$, $MnSO_4$, and $CoSO_4$ that have been solved with gradual drops of aquadest with mol Ti:M (M= Cd, Co, Mn) ratio of 3:1. TiO_2-M gel was then heated at 150 °C for approximately 24 hours and calcined at different temperatures of 300, 400, and 500 °C for 2 hours.

2.4 Determination of Optimum pH for Solution

Some 0.1 gram of TiO_2 and TiO_2-M (T= 400 °C) was added to 10 mL solution of *Remazol Brilliant Blue R* and *Remazol Yellow FG* 10 ppm at different pH of 3, 5, 7, 9, and 11. The solution was stirred and raid with visible light for 30 minutes at the black box reactor. The solution was filtered with *Whatmann 42* and tested with a UV-Vis spectrophotometer.

2.5 Determination of Optimum Catalyst Phase

Some 0.1 gram of TiO_2 and TiO_2-M at different temperatures of 300, 400, and 500 °C was added to 10 mL solution of *Remazol Brilliant Blue R* and *Remazol Yellow FG* 10 ppm at the optimum pH. The solution was stirred and raid with visible light for 30 minutes at the black box reactor. The solution was filtered with *Whatmann 42* and tested with a UV-Vis spectrophotometer.

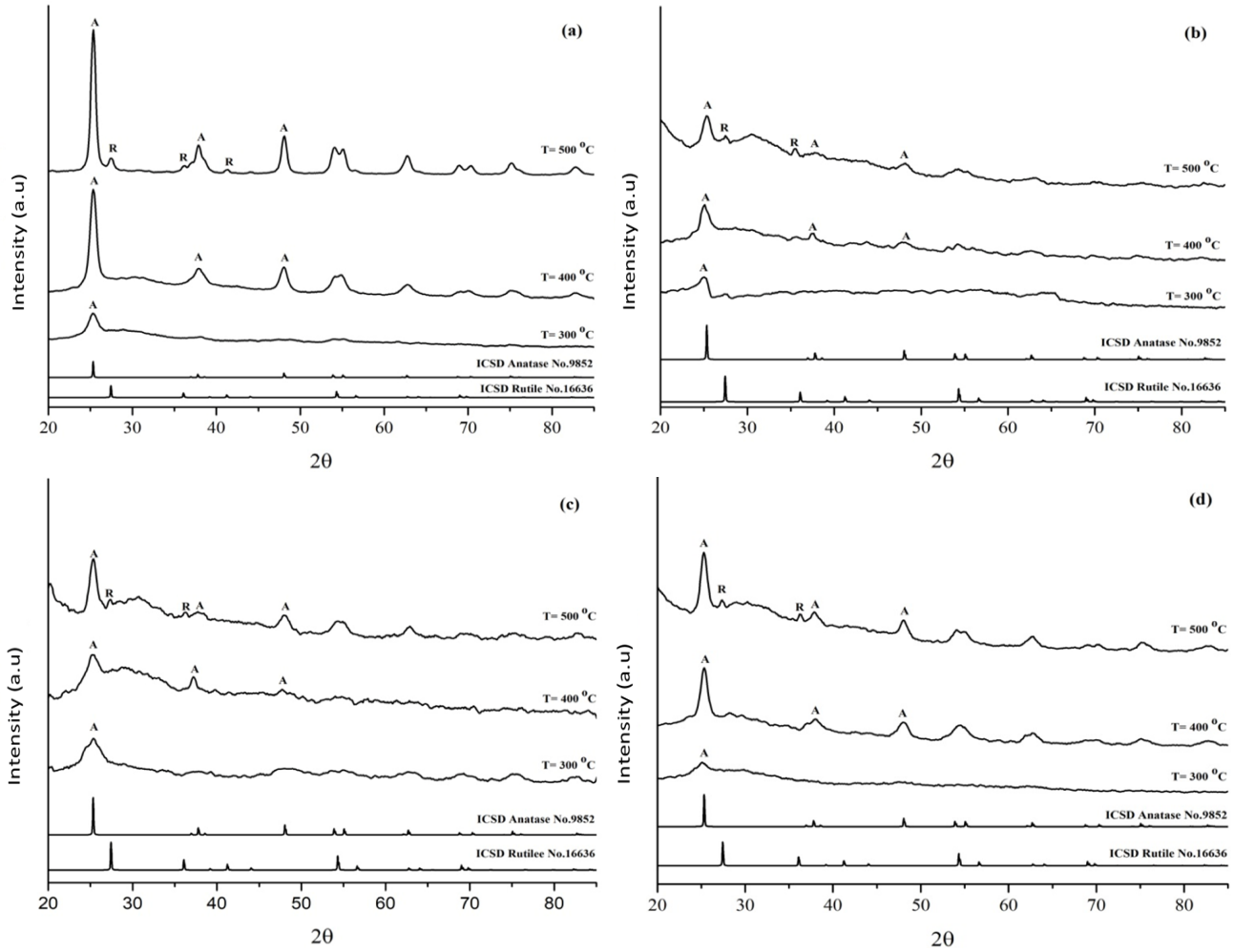

Figure 1. Patterns of XRD (a) TiO_2, (b) TiO_2-Cd, (c) TiO_2-Co, and (d) TiO_2-Mn at different calcination temperatures (300, 400, and 500 °C).

3. Results And Discussion

3.1 Characterization of XRD

The structure and size of the crystal obtained from the material can be identified through characterization with XRD. Calcination temperature and dopant will affect the formation of the crystal phase. The patterns of XRD TiO_2, TiO_2-Cd, TiO_2-Co, and TiO_2-Mn at different calcination temperatures of 300, 400, and 500 °C are shown in Figure 1.

TiO_2 and TiO_2-M diffractogram for different calcination temperatures resulted in different diffraction patterns. Diffraction patterns showed the transformation from amorphous to anatase and from anatase to rutile in line with the increase of calcination temperature. At the calcination temperature of 300 °C, the formed TiO_2 and TiO_2-M (Cd, Co, Mn) were more likely to be amorphous. At the calcination temperature of 400 °C, it was shown that in TiO_2, an anatase phase was formed. It was characterized by the appearance of a peak at 2θ = 25.4604°; 37.8755°; and 48.0653°. At TiO_2-Cd, the peak appeared at 2θ = 24.8747°; 37.5241°; and 47.9482°. At TiO_2-Co the peak appeared at 2θ = 25.2261°; 37.2899°; and 47.9482°, and at TiO_2-Mn the peak appeared at 2θ = 25.3432°; 38.2269°; and 47.9482°. The peaks resulted from the anatase in line with the ICSD Anatase No.9852. At calcination temperature of 500 °C, besides the formation of anatase phase, the rutile phase appeared as characterized by the appearance of a peak at TiO_2 at 2θ = 27.4765°; 36.9517°; and 41.2682°. At TiO_2-Cd the peak appeared at 2θ = 27.6739° and 36.8227°. At TiO_2-Co a peak appeared at 2θ = 27.258° and 36.3029°, and at TiO_2-Mn a peak appeared at 2θ = 27.362° and 36.1989°. The result of XRD showed that the calcination temperature of 400 °C was the optimum temperature in the formation of the anatase phase. Therefore, when calcination temperature is lower, the amorphous form is likely to be formed and when calcination temperature is higher, the anatase phase starts to be unstable and transformation to rutile phase occurs. Besides that, diffraction patterns of TiO_2 and TiO_2-M (Cd, Co, Mn) show higher calcination temperature leading to a higher and sharp peak, because higher calcination temperature affects the development of the formed crystal and affect the crystallinity of TiO_2 as reported by Behnajady *et al.* [22]. The resulting diffraction pattern matches the standard, but the peak pattern shows a slight shift due to the doping effect [23]. Crystalinity is also can be affected by radius of ion metal. Ions metal Ti^{4+}; Co^{2+}; Mn^{2+}; and Cd^{2+} consecutively have a radius of 0.745 Å; 0.79 Å (ls) or 0.885 Å (hs); 0.81 Å (ls) or 0.97 Å (hs); and 1.09 Å. And overall, the crystallinity of TiO_2 is higher than metal-doped TiO_2. This is because the presence of metal dopant ions disrupts the formation of TiO_2 polymers and decrease crystal regularity or crystallinity of the catalyst. It can be seen from decreasing peak at 2θ = 25.4604° dan increasing amorphous at 2θ = 25.4604° until 37.8755°. The sizes of TiO_2 and TiO_2-M crystals can be identified through the calculation using Debye-Scherrer's equation. The sizes of the resulted crystals are shown in Table 1.

Metal doping results in the decreased size of crystal because the addition of dopant has resulted in the inhibition of TiO_2 crystal growth [24]. With different temperatures of calcination, the size of the crystal increases along with the increase of calcination temperature. Higher calcination temperature results in the formation structure of Ti−O−Ti and O−Ti−O become longer. This results in a larger volume of crystal that results in a larger size of a crystal. Crystal size is also can be affected by radius of ion metal. Ions metal Co^{2+}; Mn^{2+}; and Cd^{2+} consecutively have a radius of 0.79 Å (ls) or 0.885 Å (hs); 0.81 Å (ls) or 0.97 Å (hs); and 1.09 Å. The larger the metal ion radius, the larger the crystal size obtained. If the radius of the doping ion increases, the crystal lattice changed. The modified lattice changes the volume of the crystal cell. The larger the radius of the doping ion, the wider the lattice spacing and causes 2θ to smaller. In overall, the crystal size of TiO_2 is larger than metal-doped TiO_2. This is because

Table 1. Sizes of TiO_2 and TiO_2-M (M= Cd, Co, Mn) crystals.

Material	Size of Crystal (nm) at		
	300 °C	400 °C	500 °C
TiO_2	7.155	11.918	12.891
TiO_2-Cd	5.590	11.577	11.639
TiO_2-Mn	5.312	10.646	10.930
TiO_2-Co	4.298	6.221	9.456

the presence of metal dopant ions disrupts the formation of TiO_2 polymers and causes the size of TiO_2 macromolecules to become smaller.

The mechanism of metal ion doping into TiO_2 crystals as shown in Figure 2. The metal ion doping mechanism can be through substitutional doping (a,b) and/or Interstitial doping (c).

3.2 Characterization of SEM-EDX

Results of SEM and EDX analysis are shown in Figure 3. Results of SEM analysis in Figure 3(a) show that TiO_2 has a homogenous and regular spherical structure. The result of SEM analysis of TiO_2-M (M=Cd, Co, Mn) is shown in Figure 3(b), (c), and (d). The result of SEM shows that morphologically, TiO_2-M (M=

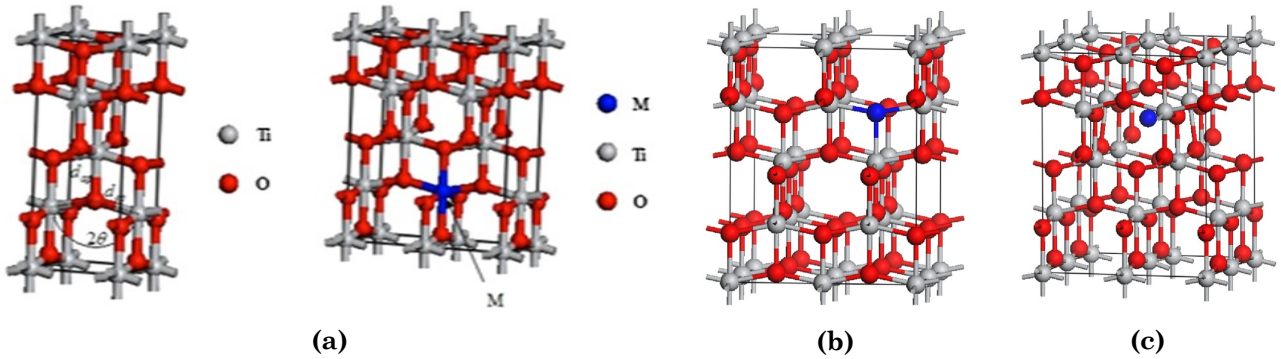

Figure 2. Mechanism of metal ion doping into TiO_2 crystals: (a), (b). substitutional doping [25], (c). Interstitial doping [26]. Blue color (M = Co, Mn, or Cd).

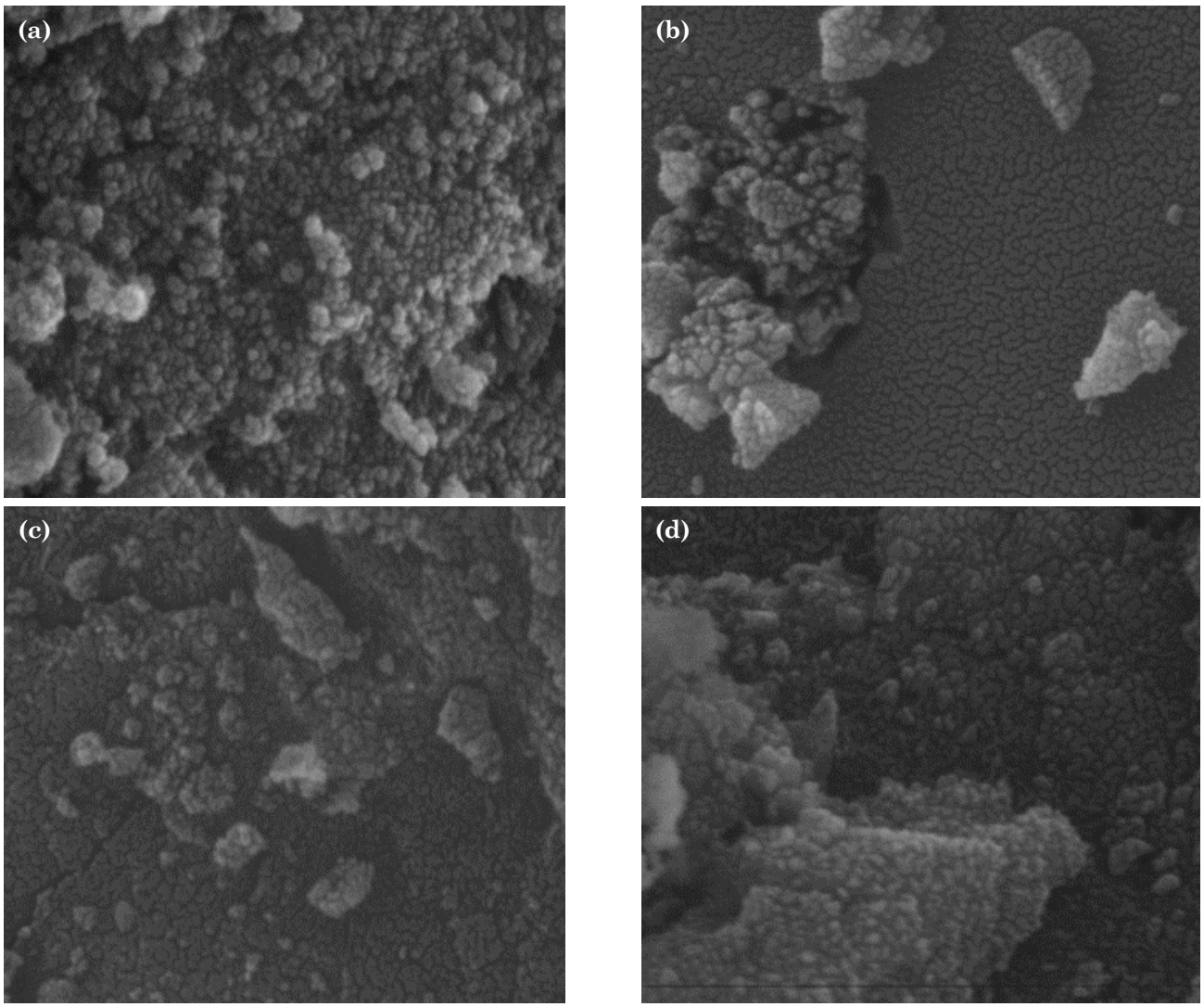

Figure 3. Morphology of (a) TiO_2 (b) TiO_2-Cd (c) TiO_2-Co (d) TiO_2-Mn.

Cd, Co, Mn) has a smoother surface than the TiO_2, because the addition of metal ion to TiO_2 may cover some parts of the surface of TiO_2-M and make them smoother.

The result of EDX shows that the material of TiO_2 comprises Ti and O, while TiO_2-M (Cd, Co, Mn) comprises Ti, O, and metal dopant. This shows that the synthesis of TiO_2-M (Cd, Co, Mn) has been successfully carried out due to the existence of the Cd, Co, Mn in the material of TiO_2-M. The percentage of Cd; Co; and Mn in the material of TiO_2-M (Cd, Co, Mn) are 10.11%; 3.42%; and 4.71%, respectively.

3.3 Energy of Band Gap

The energy of the band gap (*Eg*) is required by an electron to experience an excitation from the valence band to the conduction band [27]. The energy of the band gap can be calculated with the *Tauc* Plot method by extrapolating the correlation graph between $h\nu$ as the abscissa of axis x and $(\alpha h\nu)^2$ as the ordinate of axis y. *Tauc* Plot graph for TiO_2 and TiO_2-M (M= Cd, Co, Mn) at the calcination temperature of 300; 400; and 500 °C is shown in Figure 4. Metal ion doping results in the decreased energy of the band gap. The scores of the energy of the band gap for TiO_2 and TiO_2-M at different calcination temperatures are shown in Table 2.

The radius of the metal ion affects the resulted energy of the band gap. The larger the metal ion radius of dopant, the larger the crystal size obtained and then the higher the bandgap obtained. Band gap energy of TiO_2-Co<TiO_2-Mn<TiO_2-Cd. Ion Ti^{4+} has a radius of 0.745 Å, while ion Co^{2+}; Mn^{2+}; and Cd^{2+} consecutively have a radius of 0.79 Å (ls) or 0.885 Å (hs); 0.81 Å (ls) or 0.97 Å (hs); and 1.09 Å. When the radius of metal dopant ion reaches a radius of ion Ti^{4+}, the formation of inter band gap level becomes much easier, so that it

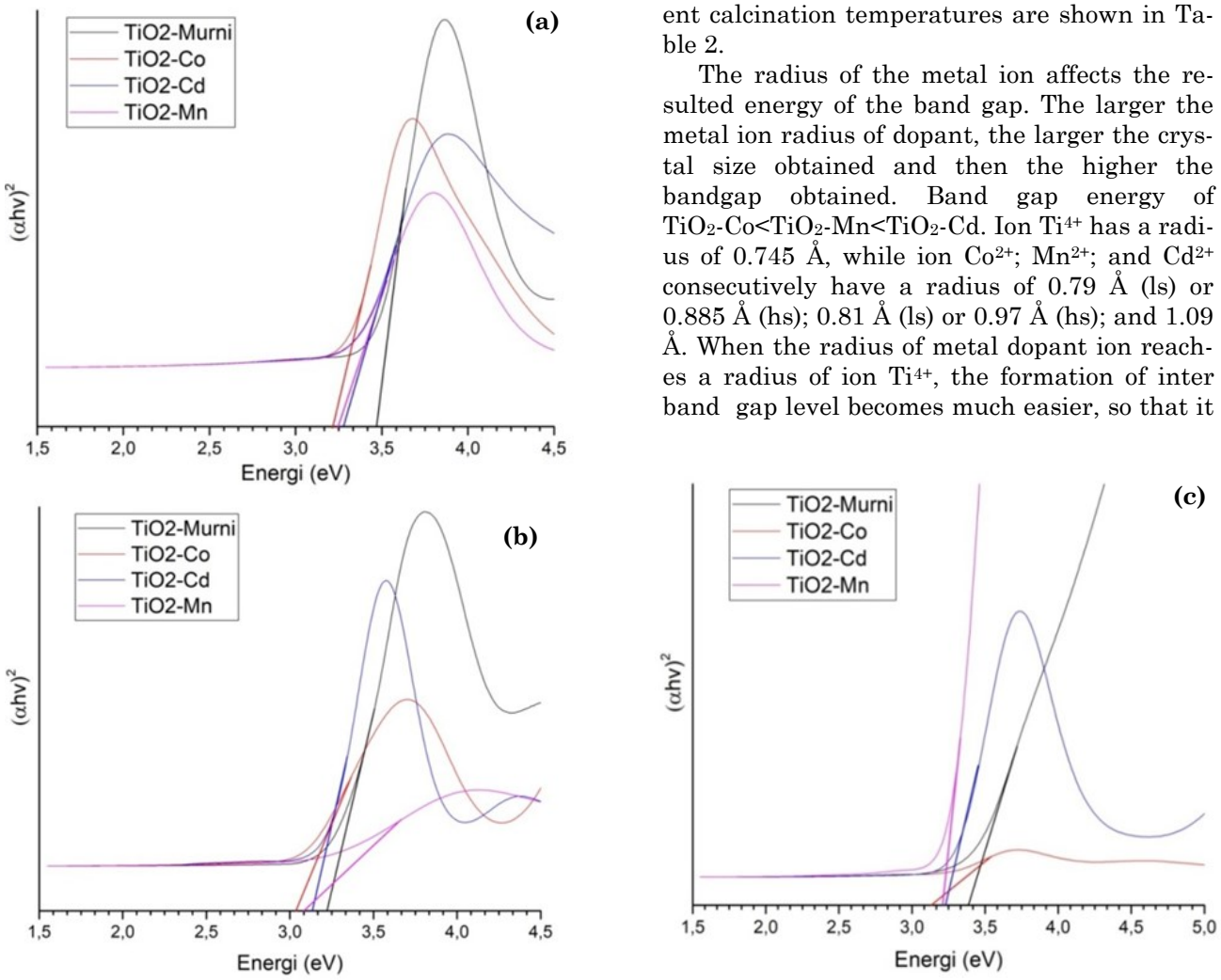

Figure 4. *Tauc* Plot Graph of TiO_2 and TiO_2-M (M=Cd, Co, Mn) (a) T = 300 °C, (b) 400 °C, (c) T = 500 °C

Table 2. Scores of the energy of band gap for TiO_2 and TiO_2-M at the calcination temperature of 300, 400, and 500 °C.

Sample	Energy of band gap (eV) at		
	T = 300 °C	T = 400 °C	T = 500 °C
TiO_2	3.48 eV	3.28 eV	3.39 eV
TiO_2-Cd	3.31 eV	3.18 eV	3.26 eV
TiO_2-Mn	3.30 eV	3.10 eV	3.23 eV
TiO_2-Co	3.26 eV	3.04 eV	3.18 eV

results in the decrease of band gap energy of the material as reported by Chen *et al.* [28]. The radius of metal ion Co^{2+} is more close to the radius of ion Ti^{4+}, so that it results in the smallest bandgap energy.

Calcination temperature also affects the magnitude of band gap energy. At the calcination temperature of 300 °C the band gap energy is largest because, at the temperature, an amorphous phase is likely to be formed. Amorphous TiO_2 does not have a regular valence band and conduction band. Therefore, the bandgap energy is large. Band gap energy at the calcination of 500 °C is higher than at 400 °C because at 500 °C, the rutile phase is formed and it results in irregularity of TiO_2 or non-uniform TiO_2. In addition, the greater the calcination temperature, the size of the catalyst crystals formed is larger so that the band gap becomes larger.

3.4 Determination of Optimum pH of a Solution

According to Goswami *et al.* [21], photocatalytic degradation is divided into two stages, namely adsorption and degradation. In the initial stage, TiO_2 absorbs dye molecules and in the second stage the dye decomposes after irradiation. The photocatalytic reaction of TiO_2 consists of photoreduction and photooxidation reactions initiated by the adsorption of the substrate on the surface. The degradation mechanism of Remazol Brilliant Blue R and Remazol Yellow FG using TiO_2–M (Co, Cd, Mn) is written as follows:

$$TiO_2\text{–}M + h\nu \rightarrow e_{cb}^- + h_{vb}^+ \quad (1)$$

$$O_2 + e^- \rightarrow \cdot O_2^- \quad (2)$$

$$\cdot O_2^- + H^+ \rightarrow HO_2\cdot \quad (3)$$

$$2HO_2\cdot \rightarrow O_2 + H_2O_2 \quad (4)$$

$$e^- + H_2O_2 \rightarrow OH^- + \cdot OH \quad (5)$$

$$OH^- + h^+ \rightarrow \cdot OH \quad (6)$$

$$h^+ + H_2O \rightarrow H^+ + \cdot OH \quad (7)$$

Remazol Brilliant Blue R + $\cdot OH \rightarrow$ smaller degradation product $\rightarrow CO_2 + H_2O + SOx + NOx$ (8)

Remazol Yellow FG + $\cdot OH \rightarrow$ smaller degradation product $\rightarrow CO_2 + H_2O + SOx + NOx$ (9)

Remazol Brilliant Blue R + $\cdot O_2^- \rightarrow$ smaller degradation product $\rightarrow CO_2 + H_2O + SOx + NOx$ (10)

Remazol Yellow FG + $\cdot O_2^- \rightarrow$ smaller degradation product $\rightarrow CO_2 + H_2O + SOx + NOx$ (11)

If TiO_2 is given the appropriate energy there will be an excitation of electrons from the valence band (VB) to the empty conduction band (CB) and leaves a hole (h^+) in the valence band as a positive charge. Electrons react with O_2 to form superoxide radicals ($\cdot O_2^-$) and the holes formed react with H_2O in solution to form hydroxyl radicals ($\cdot OH$). Hydroxyl radicals and superoxide radicals continue to be formed during the irradiation process and degrade the dye into simpler components.

Different pH in solutions can affect the charge of TiO_2 surface and affect the structure of dyes that have impacts on the process of photodegradation. At the acid pH, surface TiO_2 have a positive charge, while at alkaline pH, it have a negative charge. Anionic dyes of *Remazol Brilliant Blue R* and *Remazol Yellow FG* in acid condition have a strong anionic character. Therefore, the two dyes experience a stronger

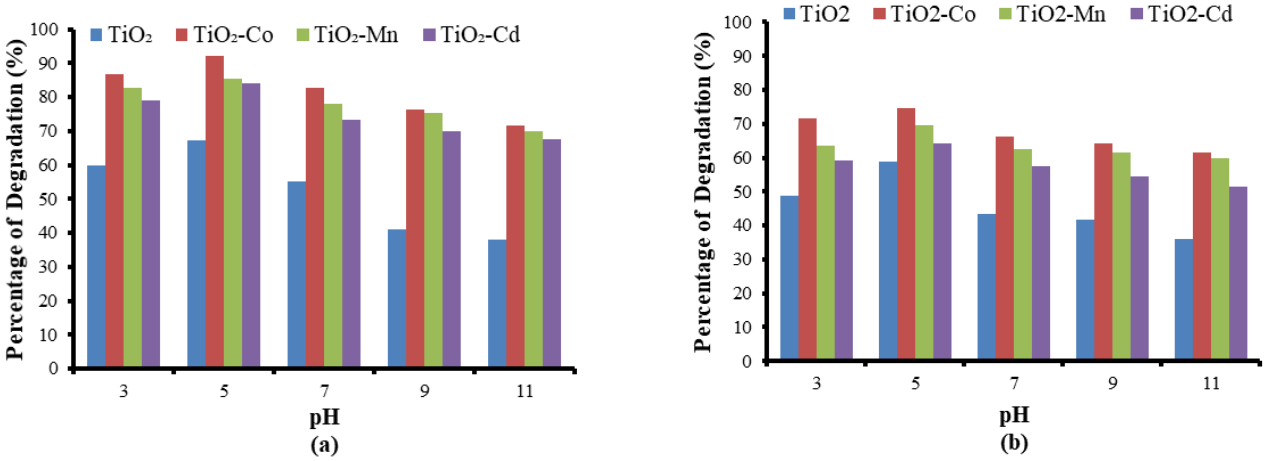

Figure 5. Degradation Percentage for (a) *Remazol Brilliant Blue R* (b) *Remazol Yellow FG* using TiO_2, TiO_2-Co, TiO_2-Mn, and TiO_2-Cd at different pHs.

electrostatic interaction at acid pH due to the different charges between the dyes and the surface.

Based on the result of the analysis in Figure 5, it is known that the optimum pH of both dyes is obtained at pH 5. This shows that *Remazol Brilliant Blue R* and *Remazol Yellow FG* have effective degradation at the acid pH and decreases along with the increase of pH. At acid pH, the hydroxyl radical resulting from the photocatalyst system becomes even higher. In acidic conditions there is an increase in H^+ ions in the solution. At acidic pH the hydroxyl radicals produced by the photocatalyst system increase with the following equation.

$$e^- + O_2 \rightarrow \cdot O_2^- \quad (12)$$
$$\cdot O_2^- + H^+ \rightarrow HO_2\cdot \quad (13)$$
$$2HO_2\cdot \rightarrow O_2 + H_2O_2 \quad (14)$$
$$e^- + H_2O_2 \rightarrow OH^- + \cdot OH \quad (15)$$
$$h^+ + OH^- \rightarrow \cdot OH \quad (16)$$

As reported by Sibarani *et al.* [29], at an acidic pH the decomposition process of H_2O_2 in producing hydroxyl radicals occurs quickly, because OH^- will bind to H^+ so that it will increase the number of hydroxyl radicals that play a role in the degradation process of Remazol Brilliant Blue R and *Remazol Yellow FG*. Besides that, at acid pH, hydrogen radical (•H) will also be formed. Hydrogen radicals can degrade dyes. The reaction of •H formation is shown in the following equation:

$$e^- + H^+ \rightarrow \cdot H \quad (17)$$

The formation of hydroxyl radical and hydrogen radical results in higher effectivity of degradation of *Remazol Brilliant Blue R* and *Remazol Yellow FG* at acid pH than the alkaline pH. Under alkaline conditions, the decomposition of H_2O_2 is inhibited due to the concentration of $\cdot OH^-$ from the solution. A similar study was also reported by El-Bahy *et al.* [30] where the degradation process of Direct Blue 53 anionic dye using TiO_2-Gd in the pH range of 2-9 resulted in the greatest degradation efficiency at pH 4 which then decreased with increasing pH.

The degradation percentages of *Remazol Brilliant Blue* R at pH 5 are 67.34% (TiO_2), 92.12% (TiO_2-Co), 85.47% (TiO_2-Mn), and 83.91% (TiO_2-Cd), while for *Remazol Yellow FG* they are 58.84 % (TiO_2), 64.19% (TiO_2-Cd), 74.61% (TiO_2-Co), and 67.93% (TiO_2-Mn). Photocatalytic activity of TiO_2-M is better than TiO_2. This is correlated to the bandgap energy of TiO_2-M that is smaller than TiO_2, where the smaller bandgap energy of material will lead to a larger percentage of degradation.

3.5 Determination of Optimum Catalyst Phase

The catalyst phase affects the degradation of *Remazol Brilliant Blue R,* where it is known that the anatase phase has high photocatalytic activity. According to Kiswanti & Pratapa [31], the formation of the crystal phase is affected by calcination temperature. The result of the degradation of *Remazol Brilliant Blue R* and *Remazol Yellow FG* with different catalyst phases is shown in Figure 6.

Figure 6 shows that the degradation of *Remazol Brilliant Blue R* and *Remazol Yellow FG* reach the highest level at the anatase phase, because the anatase phase is the most photoactive phase and the formation of free radicals is higher in the crystal at the anatase

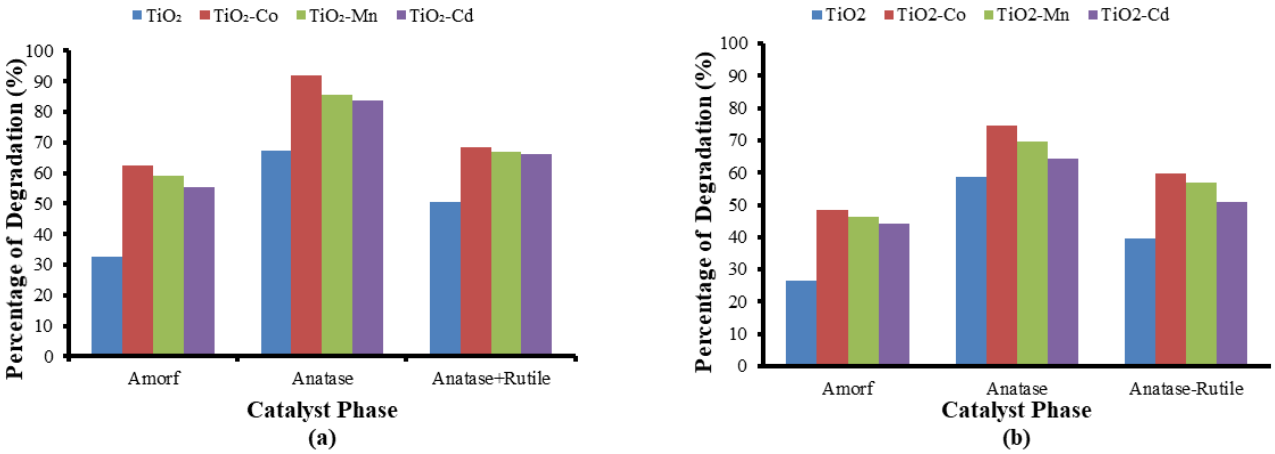

Figure 6. Degradation Percentage for (a) *Remazol Brilliant Blue R* (b) *Remazol Yellow FG* using TiO_2, TiO_2-Co, TiO_2-Mn, and TiO_2-Cd at different catalyst phases.

phase than in rutile phase [32]. At the amorphous phase, the lowest result is found because at the amorphous phase, an active site from the catalyst has not been perfectly formed. Accordingly, the photocatalytic activity is low. The anatase phase is the most photoactive phase, because it has a larger surface area when compared to the rutile phase [33]. In the rutile phase, lower yields were obtained when compared to the anatase phase. This is because the rutile phase has a lower photocatalytic activity and causes a decrease in the degradation product. In the amorphous phase, the lowest yield was obtained, because in the amorphous phase the active site had not been completely formed, so the photocatalytic activity was low. The results of a similar study were also reported by Subagja *et al.* [34], where TiO_2 in the anatase and rutile phases was obtained with a calcination temperature of 400 °C to 600 °C and resulted in the highest percentage of Methyl Orange degradation in the dominant anatase phase and decreased along with the formation of the rutile phase.

Results of degradation of *Remazol Brilliant Blue R* and *Remazol Yellow FG* show that *Remazol Brilliant Blue R* has a higher percentage of degradation. This is closely related to the different structures of the two dyes. *Remazol Brilliant Blue R* has a molecular mass of 626.53 gram/mol, while *Remazol Yellow FG* has 659 gram/mol. The different molecular mass results in an easier process of degradation of *Remazol Brilliant Blue R* because it has a smaller molecular mass than *Remazol Yellow FG* and consequently, it is more easily degraded and has a higher percentage of degradation.

This is also caused by the different structures of the two dyes. The structure of the two dyes. Analysis of the structure of both dyes shows that the structure of *Remazol Brilliant Blue R* has more phi (π) and double bonds than *Remazol Yellow FG*. Double bonds at the base structure of a compound contribute to resulted color. The double bonds are unstable. Accordingly, the bonds are easily attacked by hydroxyl radical (•OH), which is strong oxidation to become a simple component. A larger number of double bonds of a dye result in a higher sensitivity to the oxidation to the carotenoid compound as reported by Susilowati & Januar [35]. Besides that, *Remazol Brilliant Blue R* has an amine cluster at the orto and meta position so that the *steric hindrance effect* is larger and more reactive. This has resulted in higher degradation of *Remazol Brilliant Blue R* than *Remazol Yellow FG*. Hydroxyl radical is the primary radicals that initiate the degradation of dye compounds. The proposed of the degradation reaction of Remazol Brilliant Blue R

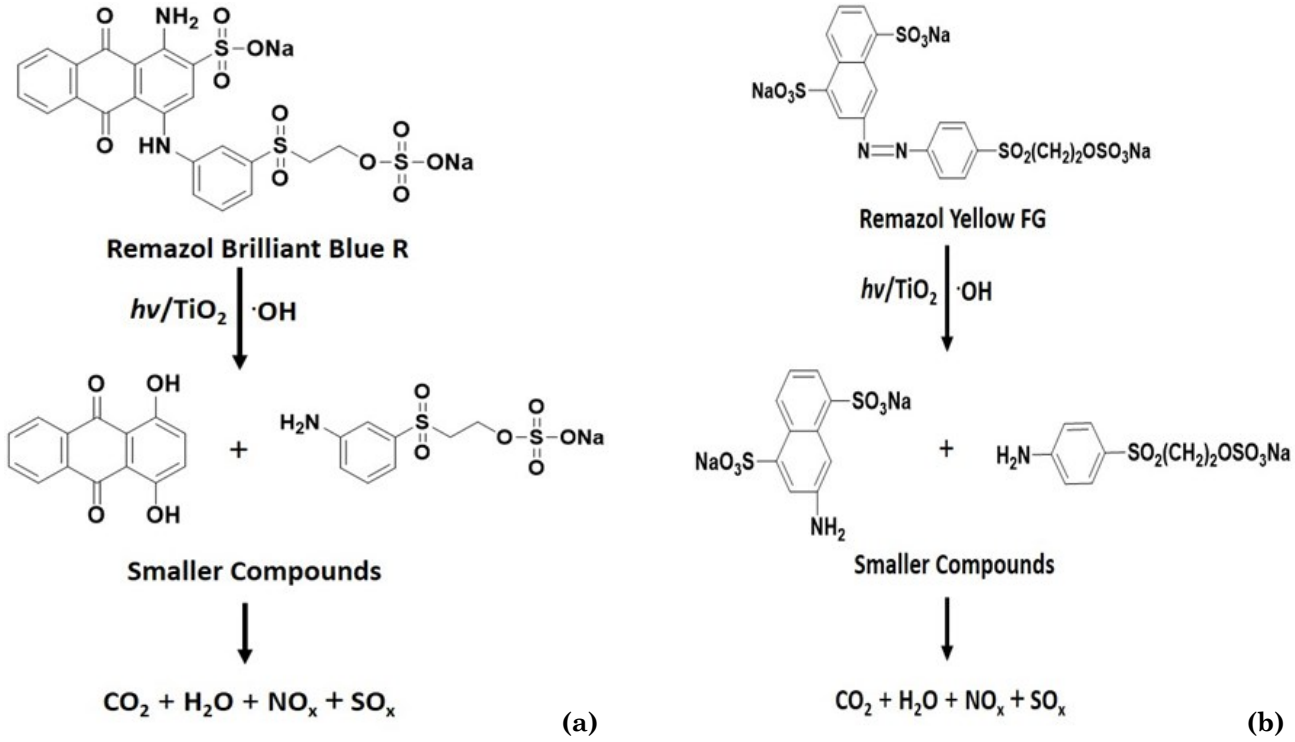

Figure 7. Mechanism of the degradation reaction of (a). *Remazol Brilliant Blue R* and (b). *Remazol Yellow FG*.

and Remazol Yellow FG as shown in Figure 7, while the graphical abstract of the research is shown in Figure 8.

4. Conclusion

Catalyst TiO_2 and TiO_2 doped Cd, Co, Mn (TiO_2-M) were synthesized with a sol-gel method, and the photocatalytic activity of *Remazol Brilliant Blue R* and *Remazol Yellow FG* has been conducted. The radius of the metal ion (Co^{2+} = 0.79Å; Mn^{2+} = 0.81Å; Cd^{2+} = 0.109Å) affects the crystallinity, Crystal size, and band gap the catalyst. Overall, the crystallinity of TiO_2 is higher than metal-doped TiO_2. The larger the metal ion radius, the larger the crystal size obtained. The larger the metal ion radius, the higher the band gap obtained which is band gap energy of TiO_2-Co<TiO_2-Mn<TiO_2-Cd.

TiO_2 and TiO_2-M at the calcination temperature of 400 °C have the best characteristics since their optimal anatase phase is formed and has lower band gap energy. The optimum degradation of *Remazol Brilliant Blue R* and *Remazol Yellow FG* is reached at acid pH (pH 5) with anatase phase. The percentages degradation of *Remazol Brilliant Blue R* were 67.34% (TiO_2), 92.12% (TiO_2-Co), 85.47% (TiO_2-Mn), and 83.91% (TiO_2-Cd), while for *Remazol Yellow FG* they were 58.84% (TiO_2), 64.19% (TiO_2-Cd), 74.61% (TiO_2-Co), and 67.93% (TiO_2-Mn), respectively.

Acknowledgement

The authors gratefully acknowledge the financial support from the Ministry of Education, Culture, Research and Technology, Republic of Indonesia via *Hibah Riset Fundamental* – PNBP Sebelas Maret University (UNS) 2018 with contract number 543/UN.27.21/PP/2018.

References

[1] Routoula, E., Patwardhan, S.V. (2020). Degradation of Anthraquinone Dyes from Effluents: A Review Focusing on Enzymatic Dye Degradation with Industrial Potential. *Environ. Sci. Technol.*, 54, 647–664. DOI: 10.1021/acs.est.9b03737.

[2] Saputra, O.A., Kurnia, K., Pujiasih, S., Rizki, V.N., Nurhayati, B., Pramono, E., Purnawan, C. (2020). Silylated-montmorillonite as co-adsorbent of chitosan composites for methylene blue dye removal in aqueous solution. *Commun. Sci. Technol.*, 5, 45–52. DOI: 10.21924/cst.5.1.2020.182.

[3] Hariani, P.L., Faizal, M., Ridwan, R., Marsi, M., Setiabudidaya, D. (2018). Removal of Procion Red MX-5B from songket's industrial wastewater in South Sumatra Indonesia using activated carbon-Fe3O4 composite. *Sustain. Environ. Res.*, 28, 158–164. DOI: 10.1016/j.serj.2018.01.004.

[4] Rethinasabapathy, M., Kang, S.M., Lee, I., Lee, G.W., Hwang, S.K., Roh, C., Huh, Y.S. (2018). Layer-Structured POSS-Modified Fe-Aminoclay/Carboxymethyl Cellulose Composite as a Superior Adsorbent for the Removal of Radioactive Cesium and Cationic Dyes. *Ind. Eng. Chem. Res.*, 57, 13731–13741. DOI: 10.1021/acs.iecr.8b02764.

[5] Wijaya, K., Sugiharto, E., Fatimah, I., Sudiono, S., Kurniaysih, D. (2006). Utilisasi TiO_2-Zeolit dan Sinar UV untuk Fotodegradasi Zat Warna Congo Red. *Teknoin*, 11(3), 199–209. DOI: 10.20885/.v11i3.88.

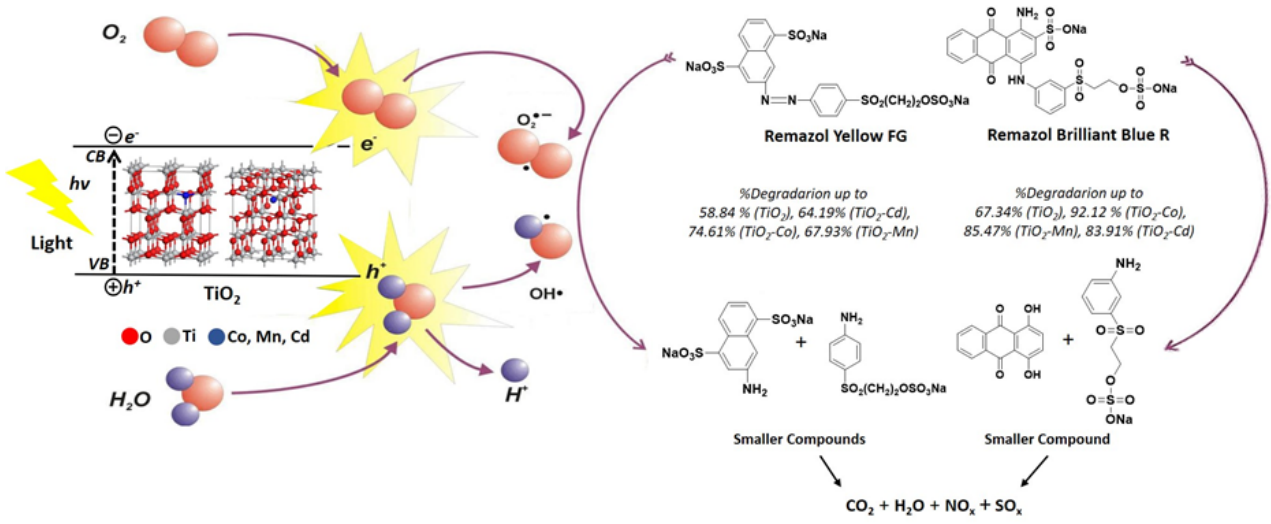

Figure 8. Graphical abstract of the research.

[6] Fatimah, I., Fadillah, G., Sahroni, I., Kamari, A., Sagadevan, S., Doong, R.A. (2021). Nanoflower-like composites of ZnO/SiO_2 synthesized using bamboo leaves ash as reusable photocatalyst. *Arab. J. Chem*., 14, 102973. DOI: 10.1016/j.arabjc.2020.102973

[7] Harjati, F., Citradewi, P.W., Purwiandono, G., Fatimah, I. (2020). Green synthesis of hematite/TUD-1 nanocomposite as efficient photocatalyst for bromophenol blue and methyl violet degradation. *Arab. J. Chem*., 13, 8395–8410. DOI: 10.1016/j.arabjc.2020.05.032

[8] Begum, S., Narwade, V.N., Halge, D.I., Jejurikar, S.M., Dadge, J.W., Muduli, S., Mahabole, M.P., Bogle, K.A. (2020). Remarkable photocatalytic degradation of Remazol Brilliant Blue R dye using bio-photocatalyst 'nano-hydroxyapatite'. *Materials Research Express,* 7, 025013. DOI: 10.1088/2053-1591/ab6f3b

[9] Mattle, M.J., Thampi, K.R. (2013). Photocatalytic degradation of Remazol Brilliant Blue by sol–gel derived carbon-doped TiO_2. *Applied Catalysis B: Environmental*, 140–141, 348–355. DOI: 10.1016/j.apcatb.2013.04.020

[10] Hanafi, M.F., Sapawe, N. (2020). Effective photocatalytic degradation of remazol brilliant blue using nickel catalyst. *Materials Today: Proceedings,* 31, 275–277. DOI: 10.1016/j.matpr.2020.05.753

[11] Suprihatin, I.E., Sibarani, J., Sulihingtyas, W.D., Ariati, K. (2019). Photodegradation of remazol brilliant blue using Fe_2O_3 intercalated bentonite. *Journal of Physics: Conference Series*, 1341, 032028. DOI: 10.1088/1742-6596/1341/3/032028

[12] Bhuiyan, M.S.H., Miah, A.Y., Paul, S.C., Aka, T.D., Saha, O., Rahaman, M.M., Sharif, M.J.I., Habiba, O., Ashaduzzaman, M. (2020). Green synthesis of iron oxide nanoparticle using Carica papaya leaf extract: application for photocatalytic degradation of remazol yellow RR dye and antibacterial activity. *Heliyon*, 6, e04603. DOI: 10.1016/j.heliyon.2020.e04603

[13] Akti, F., Balci, S. (2022). Synthesis of APTES and alcohol modified Sn/SBA-15 in presence of competitive ion: Test in degradation of Remazol Yellow. *Materials Research Bulletin,* 145, 111496. DOI: 10.1016/j.materresbull.2021.111496

[14] Akti, F. (2018). Photocatalytic degradation of remazol yellow using polyaniline–doped tin oxide hybrid photocatalysts with diatomite support. *Applied Surface Science*, 455, 931–939. DOI: 10.1016/j.apsusc.2018.06.019

[15] Khairy, M., Zakariya, W. (2014). Effect of Metal-doping of TiO_2 Nanoparticle on Their Photocatalytic Activities toward Removal of Organic Dyes. *Egyptian Petroleum Research Institute*, 23, 419–426. DOI: 10.1016/j.ejpe.2014.09.010

[16] Yan, H., Wang, X., Yao, M., Yao, X. (2013). Band Structure Design of Semiconductors for Enhanced Photocatalytic Activity: The Case of TiO_2. *Progress in Natural Science: Materials International*, 23(4), 402–407. DOI: 10.1016/j.pnsc.2013.06.002

[17] Purnawan, C., Wahyuningsih, S., Kusuma, P.P. (2016). Photocatalytic and photoelectrocatalytic degradation of methyl orange using graphite/$PbTiO_3$ composite. *Indonesia J. Chem*., 16, 347–352. DOI: 10.22146/ijc.21152.

[18] Purnawan, C., Wahyuningsih, S., Nawakusuma, V. (2018). Methyl violet degradation using photocatalytic and photoelectrocatalytic processes over graphite/$PbTiO_3$ composite. *Bull. Chem. React. Eng. Catal.,* 13, 127–135. DOI: 10.9767/bcrec.13.1.1354.127-135.

[19] Rilda, Y., Arief, S., Dharma, A., Alif, A. (2010). Modification and Characterization of Titania (M-TiO_2) by Doping Transition Metals Feni and Cuni. *Indonesian Journal of Nature*, 12(2), 178–185. DOI: 10.31258/jnat.12.2.178-185

[20] Oseghe, E.O., Ndungu, P.G., Jonnalagadda, S.B. (2015). Synthesis of Mesoporous Mn/TiO_2 Nanocomposites and Investigating the Photocatalytic Properties in Aqueous System. *Environ. Sci. Pollut. Res.*, 22, 211–222. DOI: 10.1016/j.cej.2012.02.072

[21] Goswami, P., Debnath, R.K., Ganguli, J.N. (2013). Photophysical and Photochemical Properties of Nanosized Cobalt-Doped TiO_2 Photocatalyst. *Asian Journal of Chemistry*, 25(13), 7118–7124. DOI: 10.14233/ajchem.2013.14458

[22] Behnajady, M.A., Eskandarloo, H., Modirshahla, N., Shokri, M. (2011). Sol-gel Low-Temperature Synthesis of Stable Anatase-type TiO_2 Nanoparticle Under Different Conditions and Its Photocatalytic Activity. *Photochemistry and Photobiology*, 87, 1002–1008. DOI: 10.1111/j.1751-1097.2011.00954.x

[23] Naghibi, S., Gharagozlou, M. (2017). Solvothermal Synthesis of M-doped TiO_2 Nanoparticle for Sonocatalysis of Methylene Blue and Methyl Orange (M= Cd, Ag, Fe, Ce, and Cu). *Journal of The Chinese Chemical Society*, 1(1), 1–11. DOI: 10.1002/jccs.201700013

[24] Wang, Y., Zhang, R., Li, J., Li, L., Lin, S. (2014). First-principles study on transition metal-doped anatase TiO_2. *Nanoscale Research Letters*, 9, 46. DOI: 10.1186/1556-276X-9-46

[25] Wu, H.C., Lin, Y.S., Lin, S.W. (2013). Mechanisms of Visible Light Photocatalysis in N-Doped Anatase TiO_2 with Oxygen Vacancies from GGA+U Calculations. *International Journal of Photoenergy,* 2013 (5358). DOI: 10.1155/2013/289328

[26] Almu'minin, A. S., Haryati, T., Mulyono, T. (2016). Sintesis dan Karakterisasi Film Tipis TiO_2 sebagai Pendegradasi Pewarna Tekstil Procion Red MX-8B. *Jurnal Ilmu Dasar*, 17(2), 65–72. DOI: 10.19184/jid.v17i2.2685

[27] Chen, H., Jiang, G., Jiang T., Li, L., Liu, Y., Huang, Q., Chen, W. (2015). Preparation of Mn-doped ZrO_2/TiO_2 Photocatalysts for Efficient Degradation of Rhodamine B. *MRS Communications*, 5, 525–531. DOI: 10.1557/mrc.2015.59

[28] Sibarani, J., Purba, D.L., Suprihatin, I.E., Manurung, M. (2016). Photodegradation of Rhodamine B Using ZnO/UV/Fenton's Reagent. *Journal of Applied Chemistry*, 4(1), 84–93.

[29] El-Bahy, Z.M., Ismail, A.A., Mohamed, R.M. (2009). Enhancement of Titania by Doping Rare Earth for Photodegradation of Organic Dye (Direct Blue). *Journal of Hazardous Materials*, 166, 138–143. DOI: 10.1016/j.jhazmat.2008.11.022

[30] Kiswanti, E.A.D., Pratapa, S. (2013). Synthesis of Titanium Dioxide (TiO_2) Using Acid-Dissolved Metal Method. *Jurnal Sains dan Seni Pomits*, 3(2), 18–21. DOI: 10.12962/j23373520.v3i2.6697

[31] Viana, M.M., Soares, V.F., Mohallem, N.D.S. (2010). Synthesis and Characterization of TiO_2 Nanoparticles. *Ceramics International*, 36, 2047–2053. DOI: 10.1016/j.ceramint.2010.04.006

[32] Khataee, A.R., Kasiri, M.B. (2010). Photocatalytic Degradation of Organic Dyes in the Presence of Nanostructured Titanium Dioxide: Influnce of the Chemical Structure of Dyes. *Journal of Molecular Catalysis A: Chemical*, 328, 8–26. DOI: 10.1016/j.molcata.2010.05.023

[33] Subagja, R., Royani, A., Suharyanto, A., Andriyah, L., Natasha N.C. (2014). Pengaruh Temperatur dan Waktu Kalsinasi Terhadap Perubahan Fasa TiO_2. *Majalah Metalurgi*, 29(3), 245–254. DOI: 10.14203/metalurgi.v29i3.298

[34] Susilowati, R., Januar, H.I. (2014). Temporal Variation and Physical and Chemical Stability of Brown Seaweed Carotenoid Bioactive Compounds *Turbinaria decurrens*. *JPB Perikanan*, 9(1), 21–28. DOI: 10.15578/jpbkp.v9i1.96